Rapid Variability of the Radio Flux Density of 0524 + 034

A. G. Gorshkov[1], V. K. Konnikova[1], and M. G. Mingaliev[2]

[1] Sternberg Astronomical Institute,
Universitetskiĭ prospekt 13, Moscow, 119899 Russia
[2] Special Astrophysical Observatory, Russian Academy of Sciences,
Nizhni Arkhyz, 357147 Russia

Abstract—Simultaneous observations on the RATAN-600 radio telescope at 0.97, 2.3, 3.9, 7.7, 11.1, and 21.7 GHz during the period from January 3 to February 25, 1998, revealed variability of 0524 + 034 on time scales not exceeding 10 days. The variations are correlated at all frequencies where the parameters of the variability could be determined, including in the optically thick part of the spectrum. The mean spectrum of the variable component was derived and is in agreement with the spectrum of a homogeneous, spherically symmetrical source. In the optically thin part of the spectrum, the spectral index of the variable component is $\alpha = -0.2$, reflecting the initial energy distribution of the relativistic electrons. It is argued that the variable emission is associated with the acceleration of electrons and amplification of the magnetic field and that adiabatic expansion can be neglected. It is proposed that the observed variability is due to illumination of inhomogeneities in the jet by a shock front passing through them and that the light curve reflects the distribution and characteristic sizes of these inhomogeneities (0.14–0.5 pc for angles to the line of sight not exceeding 10°, Lorentz factor $\gamma = 10$, and adopted redshift $z = 0.5$). In 0524 + 034, in addition to the rapidly variable component, there are two slowly varying components, one of which has $\alpha = -0.7$ in the optically thin part of the spectrum. © *2000 MAIK "Nauka/Interperiodica".*

1. INTRODUCTION

In [1], we reported the unusually large amplitude of the long-term flux variability of the radio source 0524 + 034 at centimeter and decimeter waves. This source was detected for the first time in 1979 in the Zelenchuk Survey, carried out on the RATAN-600 radio telescope at 8.7 GHz [2]; its flux at that time was 460 mJy. The radio source is identified with a 19th-magnitude object on the Palomar Survey O map; its 2000.0 coordinates are [3]

$$RA = 05^h27^m32^s.70, \quad DEC = 03°31'31''.44.$$

In 1996–1998, the flux density continued to increase. Over the last ten years of observations, its flux at 7.7 GHz has increased by more than a factor of 20. Here, we report the detection of flux variability on time scales shorter than 10 days at frequencies 2.3–21.7 GHz.

At centimeter wavelengths, the variability of BL Lac objects on time scales from weeks to months has been known for a long time and has been intensely studied (see, for example, [4, 5]). Variability has also been found on shorter time scales, from several hours [6] at 1.42 GHz to about one day over a wide frequency range [7]. These variations could arise within the source itself or could result from propagation of the radiation through a nonuniform medium.

If the variability is intrinsic to the source, then such short time scales for the variability result in brightness temperatures considerably exceeding the Compton limit of 10^{12} K. Therefore, the rapid variability cannot

be explained within the framework of the standard model of a spherically symmetric, homogeneous, adiabatically expanding cloud of relativistic electrons [8, 9]. Brightness temperatures exceeding the Compton limit can be explained using models with relativistic motion of the emitting plasma under a small angle to the observer's line of sight.

The behavior of variable radio sources on various time scales and over a wide frequency range can best be explained in the framework of models with shock waves propagating in relativistic plasma [10]. Our studies support such a mechanism for the variability.

2. OBSERVATIONS

Observations were carried out daily from January 3 to February 25, 1998, as part of a program to study rapid variability of sources from a complete flux-limited sample. The sample contains all sources with fluxes $S_{3.9\,GHz} > 200$ mJy near 24 h in right ascension and in the declination zone 3°30'–6°.

We included 73 sources in the observational program, among them 39 objects with flat and 34 objects with power-law spectra. We used sources with power-law spectra, which have constant fluxes, as a control group in statistical studies of the parameters of small-amplitude variability, and also for studies of instrumental effects that could result in additional errors in the flux-density determinations. The observations were carried out on the meridian on the Northern sector of
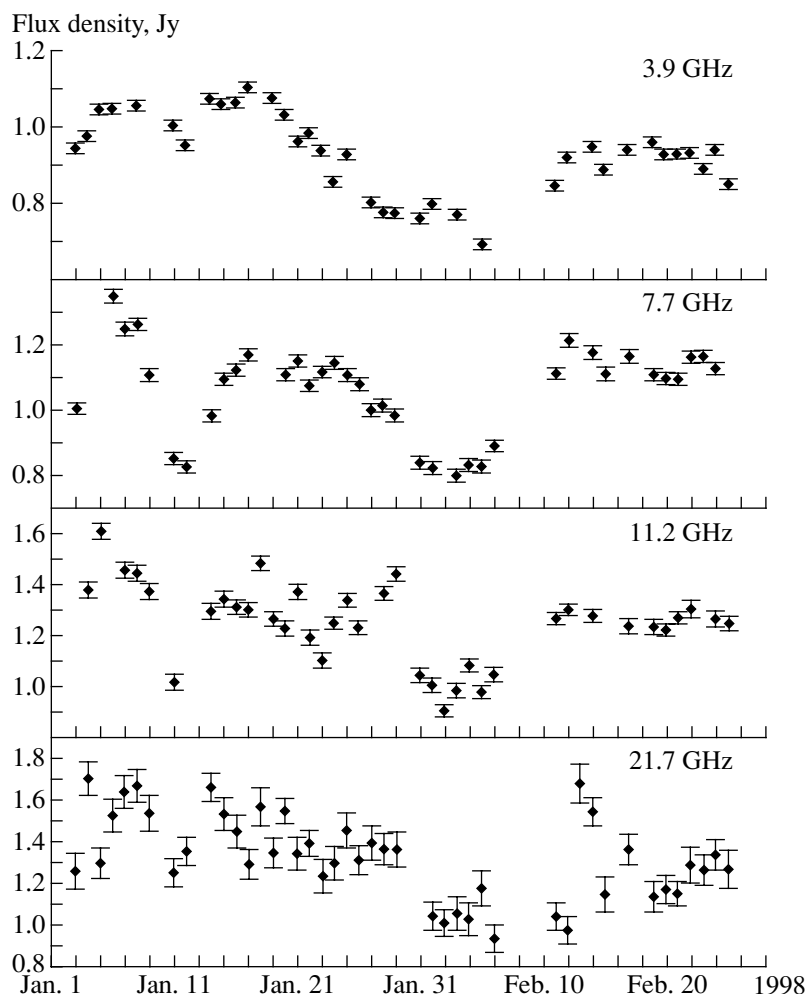
Flux density, Jy

Fig. 1. Flux densities of the source 0524 + 034 at 3.9, 7.7. 11.1, and 21.7 GHz from January 3 to February 25, 1998.

RATAN-600 in the fixed-focus regime [11], simultaneously at 0.97, 2.3, 3.9, 7.7, 11.1, and 21.7 GHz, using the standard receivers for feed no. 1. Use of the fixed-focus regime enabled us to eliminate flux errors due to displacements of the feed (secondary mirror). The parameters of the receivers and antenna beam at all frequencies are given in [12]. Using beam switching for the short-wavelength receivers at 7.7, 11.1, and 21.7 GHz enabled us to considerably reduce drifts due to atmospheric irregularities.

We matched the flux density scale to the scale for the reference sources with power-law spectra published in [13]. The data processing procedure and error estimates are described in [14].

3. RESULTS

The radio source 0524 + 034 is the only object in the sample in which we found such a large variability amplitude during the observing period. Figure 1 presents the flux densities of 0524 + 034 at 2.3, 3.9, 7.7,

11.1, and 21.7 GHz obtained during the observing session. No observations were carried out on January 10, 13, and 30 and February, 7–10, 16, and 18 due to poor weather conditions.

Considerable variability at 3.9, 7.7 and 11.1 GHz is clearly visible in the figure. This is a real effect, not an artifact, since no similar brightness curves are observed for any source from the control group. The variability index $V = \Delta S/\langle S \rangle$ was defined in [15] and represents the mean relative variability amplitude for the observing period. These indices were 0.20, 0.57, 0.76, 0.63, and 0.54 at 2.3, 3.9, 7.7, 11.1, and 21.7 GHz, respectively.

The spectrum of the source (Fig. 2) based on the mean fluxes grows toward higher frequencies. There is a minor local minimum near 7.7 GHz, testifying to the presence of at least two compact components at different stages of development in the radio source.

We studied the parameters of the variability using various methods. It proved most informative to construct the first- and second-order structure functions.

3.1. Properties of the Structure Functions

The definition of the structure functions and their basic properties are given in [16, 17]. For a measurement time series $f(t)$, the first-order and second-order structure functions $D^1(\tau)$ and $D^2(\tau)$ are defined

$$D^1(\tau) = \langle [f(t) - f(t+\tau)]^2 \rangle, \qquad (1)$$

$$D^2(\tau) = \langle [f(t+2\tau) - 2f(t+\tau) + f(t)]^2 \rangle, \qquad (2)$$

where τ is the time shift. The mth-order structure function is equal to zero for polynomials of order $m - 1$; therefore, the form of the structure function will depend only on the character of random processes and on higher order trends.

The "ideal" structure function for a random process has a characteristic appearance: two plateaus connected by a curve. For time delays larger than the longest correlation timescale for the process, the plateau amplitude $D^1(\tau)$ is equal to twice the sum of the dispersions of the instrumental noise and the process studied. For small time delays, the plateau amplitude $D^1(\tau)$ is equal to twice the dispersion of the instrumental noise. For the structure functions $D^2(\tau)$, the plateau amplitudes are equal to six times the corresponding dispersions. These plateaus are connected by a curve, whose slope depends on the nature of the process in action.

The structure function is usually represented on a logarithmic scale, so that the slope of the line connecting the two plateaus $\mu = d \log D / d \log \tau$ is determined by the power spectrum of the process $P(f)$. If $P(f) \propto f^{-1}$ (flicker noise), $D^1(\tau) \propto \tau^0$; if $P(f) \propto f^{-2}$ (shot noise), $D^1(\tau) \propto \tau^1$. In most cases, the structure function has a more complicated form, but these simple cases can be useful for analyses of radio-source variability. The presence of harmonic (or cyclic) components in the process studied decreases the magnitude of the structure function at delays comparable to the period of these components.

We constructed the structure functions $D^1(\tau)$ (Fig. 3) and $D^2(\tau)$ (Fig. 4) for all the observing frequencies. We normalized the functions to the process dispersion, which was defined

$$\sigma_{pr}^2 = \sum (f_i - \langle f \rangle)^2 / (n - 1), \qquad (3)$$

where f_i is the flux measured on the ith day and $\langle f \rangle$ is the weighted-mean flux for n days of observations. This dispersion is the sum of the variable-component dispersion σ_{var}^2 and the mean dispersion for a single measurement σ_m^2. Note that the measurement dispersion includes all sources of measurement error: instrumental noise, instability of the calibration signal, inaccuracy of the antenna pointing, etc. With this normalization, the upper plateau of the "ideal" structure function asymptotically approaches the values $\log 2$ and $\log 6$ for the
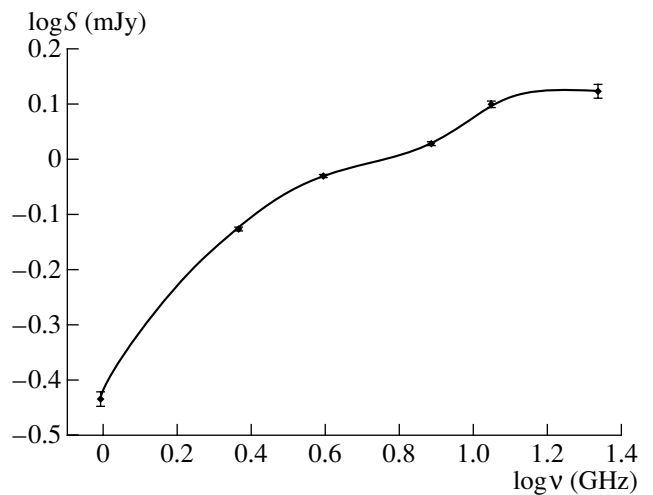

Fig. 2. The spectrum of 0524 + 034 based on the averaged data for the period from January 3 to February 25, 1998.

first- and second-order structure functions, respectively (thin horizontal lines in Figs. 3 and 4).

Both the first- and second-order structure functions for 0524 + 034 display a second plateau at 3.9, 7.7, 11.1, and 21.7 GHz. At 2.3 GHz, there are only hints of a second plateau, due to large instrumental errors and small amplitude of the variability; it is obvious that there is only instrumental noise at 0.97 GHz.

The first-order structure functions. The second plateau reaches a value of $\log 2$ for delays of 6–8 days at all frequencies. The second plateau is most obvious at 3.9 and 7.7 GHz, due to the lower instrumental noise. At 3.9 GHz, we can see a decrease of the plateau magnitude at delays longer than 20 days, with the minimum achieved at delays of about 40 days. This behavior, in combination with the fact that the plateau maximum exceeds $\log 2$, is typical of the presence of a harmonic (or cyclic) component. At the remaining frequencies, there are only hints of such a decrease.

One characteristic feature of the structure functions is the absence of a pronounced plateau due to instrumental noise at frequencies below 21.7 GHz. This testifies to the small width of the correlation function of the variable component; its magnitude changes appreciably when the delay varies from 1 to 2 days. The plateau at 21.7 GHz is most likely connected to the poorer sensitivity of the equipment at this frequency.

The slopes μ of the structure functions at 11.1, 7.7, and 3.9 GHz are close to unity. In Fig. 3, a slope corresponding to $\mu = 1$ is indicated by an arrow.

The second-order structure functions. The behavior of the second-order structure functions is similar to that of the first-order structure functions at the corresponding frequencies. The main difference from $D^1(\tau)$ is the appearance of a clearly visible first plateau at 7.7 and 3.9 GHz; the extent of the plateau varies from two days at 7.7 GHz to three days at 3.9 GHz. The decrease
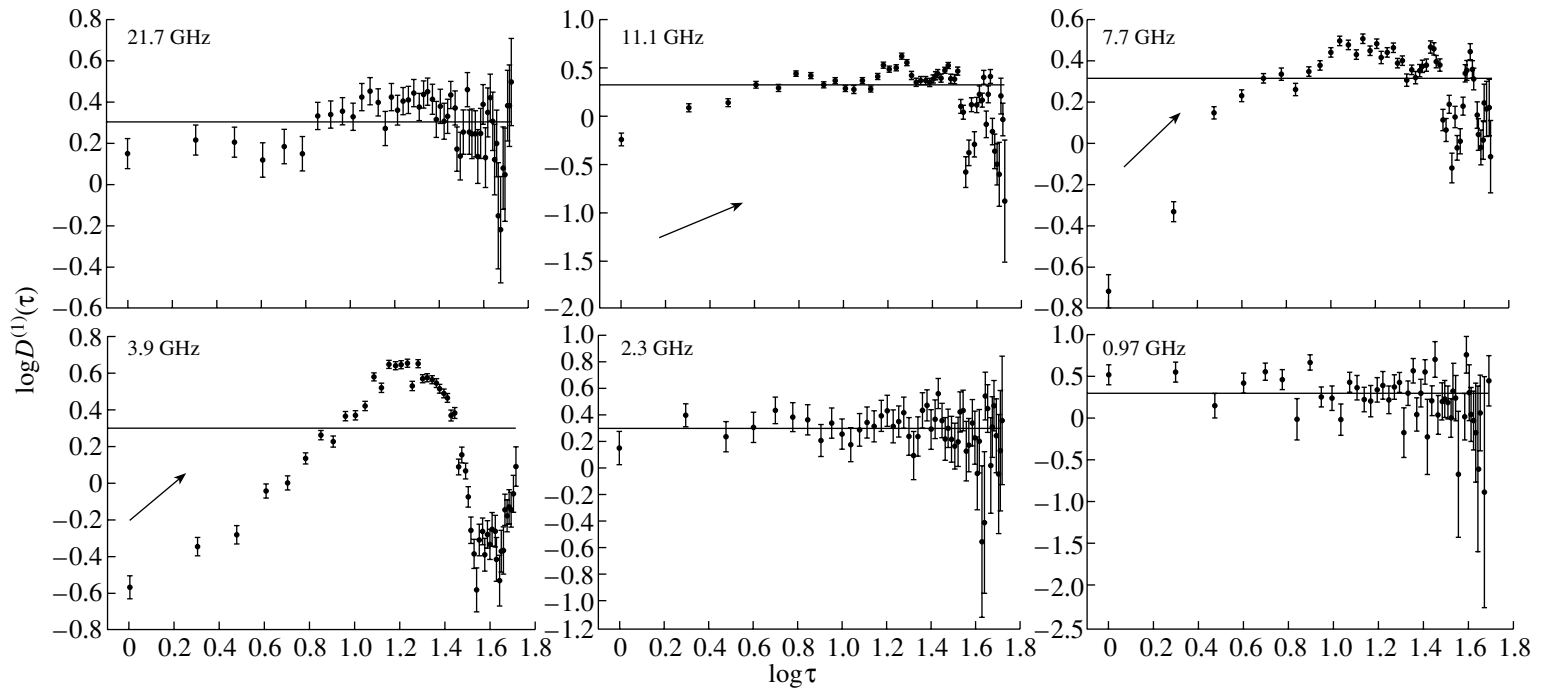
Fig. 3. The first-order structure functions $D^1(\tau)$ normalized to the dispersion on a logarithmic scale for the period from January 3 to February 25, 1998, at 0.97, 2.3, 3.9, 7.7. 11.1, and 21.7 GHz. The dashed line designates a value of $\log 2$. The arrow shows a slope corresponding to $\mu = 1$.
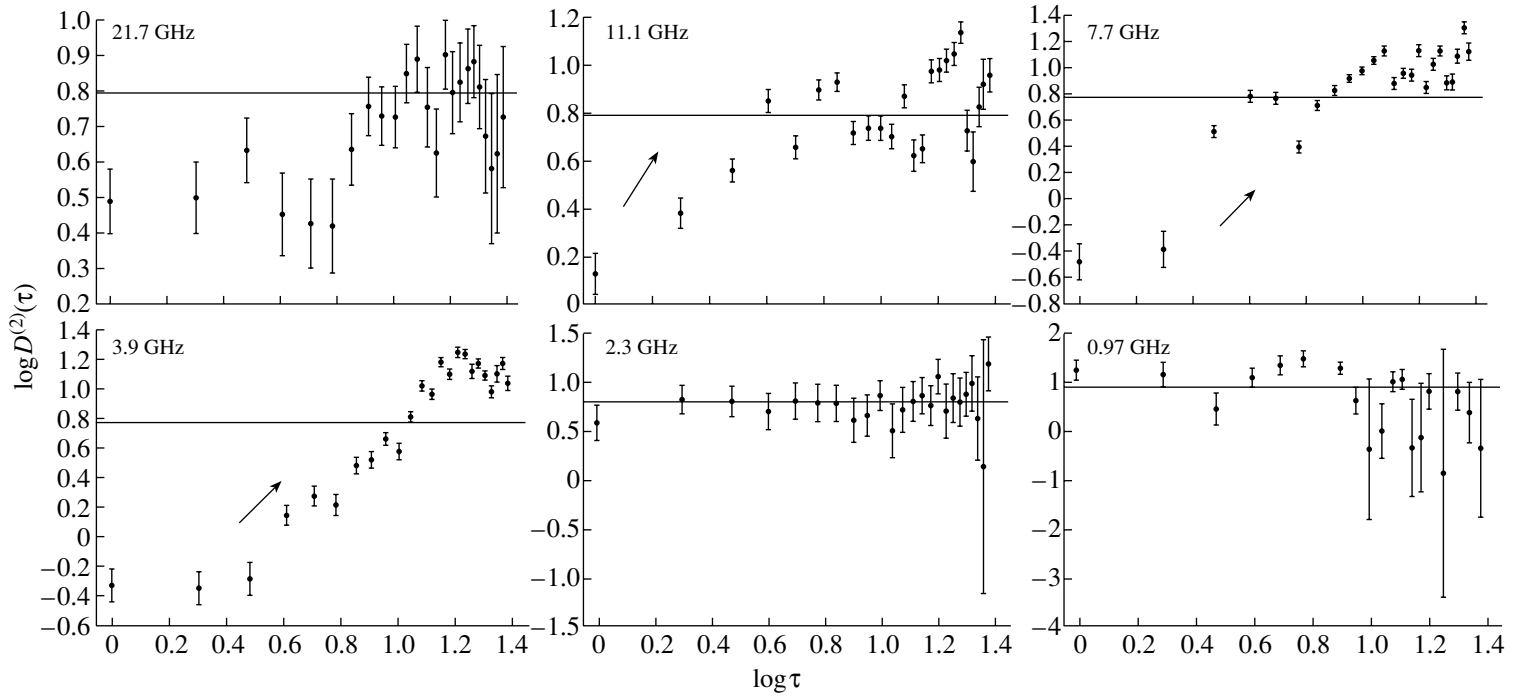
Fig. 4. The second-order structure functions $D^2(\tau)$ normalized to the dispersion on a logarithmic scale for the period from January 3 to February 25, 1998, at 0.97, 2.3, 3.9, 7.7. 11.1, and 21.7 GHz. The dashed line designates a value of $\log 6$. The arrow shows a slope corresponding to $\mu = 2$.
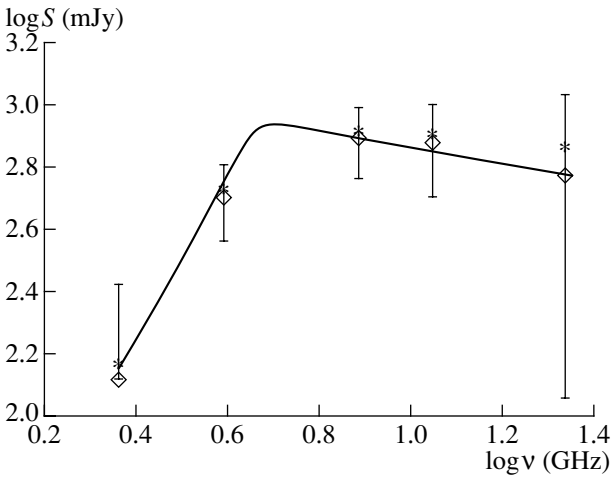
logS (mJy)

Fig. 5. The mean spectrum of the variable component of 0524 + 034 over the observation period. The diamonds show the spectrum of the flux variations, defined as $S_{var} = 6\sigma_{var}$ (the error is given for this definition of the spectrum). The asterisks show the spectrum calculated using formula (4). The solid curve corresponds to an optically thick spectral index $\alpha = 2.5$ and an optically thin spectral index $\alpha = -0.2$.

of the amplitude of the second plateau is not visible due to the halving of the maximum delay time. The slope of the structure functions is close to $\mu = 2$. For $D^2(\tau)$, this value of μ describes shot noise; in Fig. 4, this slope is also shown with an arrow.

3.2. The Frequency Spectrum of the Variations

The mean frequency spectrum of the variations for the observing period can be derived in several ways.

(1) The lower plateau of the first-order structure function (without any normalization) is twice the measurement dispersion, $2\sigma_m^2$. Hence, $\sigma_{var}^2 = \sigma_{pr}^2 - \sigma_m^2$ is the dispersion of the variable component of the radio emission. We took $D^1(1)/2$ for the value of σ_m^2, and σ_{pr}^2 was calculated using formula (3). As noted above, the lower plateau is poorly defined in the $D^1(\tau)$ structure functions; therefore, σ_m^2 is an upper estimate of the measurement dispersion. The frequency spectrum of the flux variations, defined to be $S_{var} = 6\sigma_{var}$, is shown in Fig. 5 by the diamonds.

(2) We use the formula for the variability amplitude given in [15]:

$$S_{var} = \{(n-1)[Y-(n-1)]/\sum \sigma_i^{-2}\},$$
$$Y = \sum (S_i - \langle S \rangle)^2 / \sigma_i^2. \tag{4}$$

In this case, the dispersion of a single measurement is taken to be $\sigma_i^2 = \sigma_{iform}^2 \sigma_m^2 / \sigma_{form}^2$, where σ_{iform}^2 is the formal dispersion of a single measurement and σ_{form}^2 is

the mean measurement dispersion, taking into account only the instrument noise and the instability of the calibration signal. The introduction of σ_i^2 allows us to take into account the remaining errors. The resulting spectrum, which virtually coincides with the spectrum obtained using the first method, is presented in Fig. 5 by the asterisks.

The spectrum has the canonical form for a homogeneous, spherically symmetric radio source with synchrotron self absorption. The slope α ($S \propto \nu^\alpha$) in the optically thick and optically thin parts of the spectrum are 2.5 and –0.2, and the flux peaks at 5–6 GHz. In Fig. 5, a spectrum with the indicated parameters is approximated with a continuous curve. Precisely the same parameters for the mean spectrum of a flare were obtained in [18] based on the selection and analysis of 17 isolated flares at an early stage of evolution in 15 variable sources.

Usually, when determining the spectrum of a flare, the flux of the constant component is subtracted from the observed flux. This constant flux is typically taken to equal the minimum flux near the selected flare. The methods we propose for determining the flare spectrum do not involve any assumptions about the flux of the steady or slowly varying component. The derived spectrum of the variations is the mean spectrum for the 50 days of observations; the character of the structure functions testifies to the presence during this period of a process with a timescale of 6–8 days, rather than an isolated flare. In the case of an isolated flare, the slope of the structure function $D^1(\tau)$ should be considerably greater than unity. The reasons why the mean spectrum of the variations coincides with that of an isolated flare will be analyzed below.

3.3. Correlation Functions

The autocorrelation functions at 21.7 and 2.3 GHz have no significant values for any time shifts, due to the large amplitudes of the instrumental noise at 21.7 GHz and the small amplitudes of the variations at 2.3 GHz. The autocorrelation functions at 11.1 GHz (Fig. 6a) and 7.7 GHz (Fig. 6b) display a rapid drop in their amplitudes, as expected from our analysis of the structure functions. The magnitudes of the correlation functions become insignificant for time delays exceeding three days (we chose the significance level to be 2%).

The correlation function at 3.9 GHz (Fig. 6c) is an exception: Significant values persist for time delays as long as six days, and a significant anticorrelation is observed for delays of 16–22 days. The autocorrelation function at this frequency is very smooth. This behavior of the autocorrelation function, as well as that of the structure function, testify to the presence of a periodic component with a period of 35–40 days. The autocorrelation function is broader, due to the appearance of the lower plateau in the second-order structure function at this frequency.
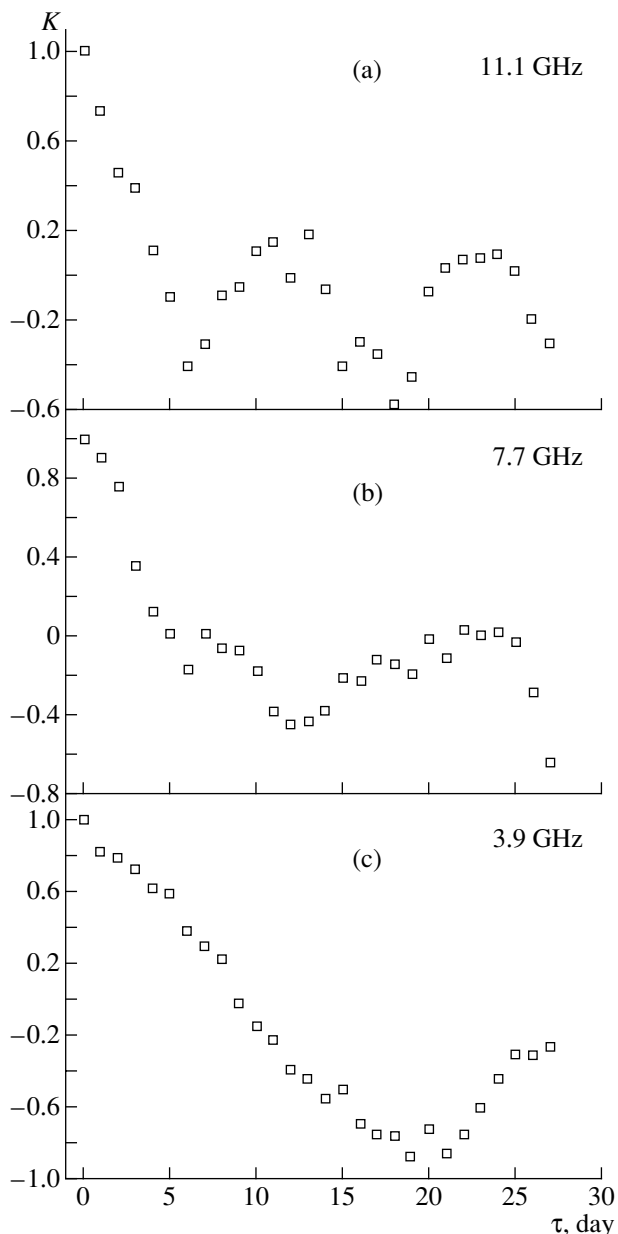
Fig. 6. Autocorrelation functions of the fluxes of 0524 + 034 at (a) 11.1, (b) 7.7, and (c) 3.9 GHz.

Fig. 7. Cross-correlation functions of the fluxes of 0524 + 034 between 11.1 and 7.7 GHz (squares) and between 7.7 and 3.9 GHz (crosses). For comparison, the autocorrelation function at 7.7 GHz (triangles) is presented.

We have constructed the cross-correlation functions for the data at 11.1–7.7 GHz and 7.7–3.9 GHz (Fig. 7). Their behavior is very similar to that of the autocorrelation functions at these frequencies. The effect of a periodic component is visible in the 7.7–3.9-GHz cross-correlation function, though it is much less pronounced than in the 3.9-GHz autocorrelation function.

Analysis of the auto- and cross-correlation functions suggests that a uniform process is responsible for flux density variations observed in the radio source 0524 + 034 at centimeter wavelengths. The small amplitud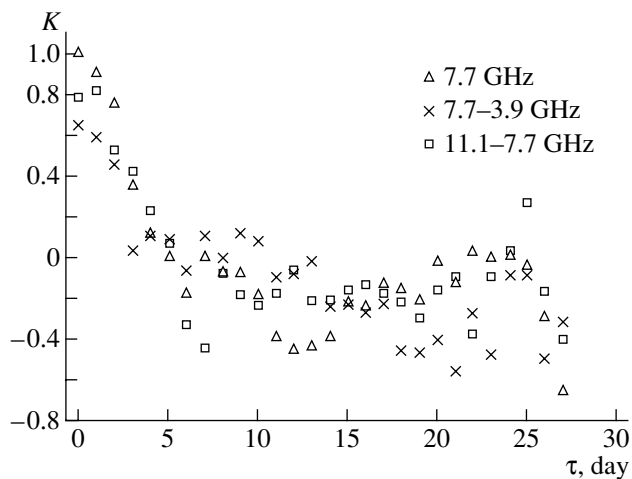e of the variations at 2.3 GHz prevents us from drawing any conclusions about the character of the variability at this frequency.

It appears that the timescale for the variations at 3.9 GHz is longer than at higher frequencies. This is no surprise, since the variations at this frequency are already observed in the optically thick part of the spectrum.

There is some inconsistency between the short time scales of the variations and the presence of a periodic component in the 3.9-GHz variations. It is possible that two processes coexist simultaneously—one with short time scales and the other with longer ones. In this picture, the development of one process is followed over the observation period. In this case, such a process could resemble a periodic process.

4. DISCUSSION

Our analysis of the cross-correlation functions indicates that the variations at 11.1, 7.7, and 3.9 GHz occur simultaneously, though the lowest frequency is already in the optically thick part of the spectrum. There is every reason to believe that the variations at 21.7 GHz are also simultaneous with those at the remaining frequencies.

The simultaneity of the variations over a broad frequency range suggest that electron acceleration and amplification of the magnetic field are important, whereas adiabatic expansion is insignificant [19]. Therefore, if the ejection of material is nonuniform along the direction of propagation of a shock, the resulting inhomogeneous structures will be illuminated when the shock passes through them, so that the light curve will reflect the distribution and characteristic sizes of the inhomogeneities. It is noted in [7] that, in shock models, the effects of expansion can be neglected
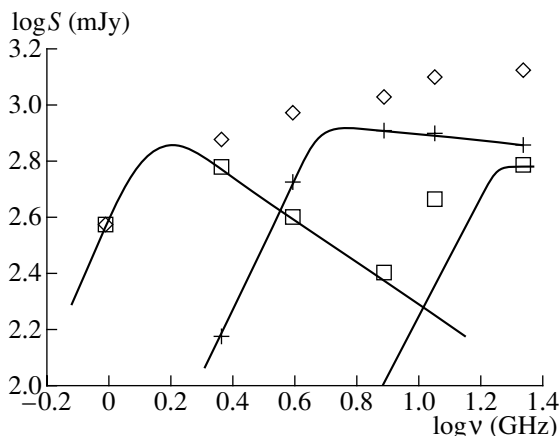
Fig. 8. Separation of the observed spectrum of 0524 + 034 into components. The diamonds show the observed spectrum. The crosses show the spectrum of the variable component; the solid curve passing through the crosses corresponds to an optically thick spectral index $\alpha = 2.5$ and an optically thin spectral index $\alpha = -0.2$. The squares show the spectrum of the slowly varying component separated into two components (solid lines); the optically thin spectral index α is -0.7.

if the jet opening angle is very small, and the sizes of the structural inhomogeneities are smaller than 1 pc. A formula relating the variation timescale to the distance covered by the shock in the jet over this time is given in [7]. For 0524 + 034, with a variation timescale of 6 days and a Lorentz factor $\gamma = 10$, this distance (the size of an inhomogeneity) is 0.14–0.5 pc for angles to the line of sight of 10° to ~0° and an adopted redshift $z = 0.5$.

In the optically thick part of the spectrum (in our case, below 5–6 GHz), the variations can be extended in time, and individual features may not coincide with those in the optically thin part of the spectrum. Precisely such a flattening could give rise to the appearance of the periodic component at 3.9 GHz, which may reflect the existence of larger inhomogeneities corresponding to variations with time scales of about 20 days.

In this case, the fact that the shape of the mean spectrum of the variations coincides with that of a spherically symmetric, homogeneous synchrotron source implies similarity of the physical conditions (electron density, electron energy distribution, and magnetic field intensity) for various inhomogeneities traversed by the shock during the observations.

Similar conclusions were drawn in [7] based on simultaneous observations of the quasar 0917 + 624 at five wavelengths spanning 2–20 cm. The timescale for the variations in 0917 + 624 is 1.3 days. The spectrum of the variations also coincides with that of a homogeneous synchrotron source, but the flux peaks at about 3 GHz and the spectral index α in the optically thin domain is –0.7. The size of the inhomogeneities is 0.16 pc for a Lorentz factor $\gamma = 14$ and angle θ close to zero. As for 0524 + 034, the spectrum of the variable compo-

nent remains virtually constant on time scales comparable to the variability timescale.

The difference in the optically-thin spectral indices of these two sources can be explained as follows. In a number of cases of long-timescale variability, the optically-thin spectrum of the variable component evolves from being flat ($\alpha = -0.2$) at an early stage to being power-law ($\alpha = -0.7$) at later stages [18]. This could be the effect of considerable radiative losses in late stages of the jet evolution. The value $\alpha = -0.2$ is typical for VLBI core components of radio sources, which are probably located close to the central engine. For noncore components, which are much more distant from the nucleus, the spectral index increases to $\alpha = -0.7$ [20].

We believe that the optically thin spectral indices of 0524 + 034 and 0917 + 624 are different because the variability is observed in components with different ages. In the former case, the variability is due to a shock propagating in a region that is close to the nucleus, and an initial electron spectrum with $\gamma = 1.4$ is observed. In the latter case, the shock is propagating in a component that is far from the nucleus, and the energetic electrons have already had time to lose some of their energy ($\gamma = 2.4$).

This interpretation is supported by the separation of the observed spectrum of 0524 + 034 into components. Since we have determined the frequency spectrum of the variations, we can remove it from the observed spectrum, yielding the spectrum of the constant or (more correctly) slowly varying component. The results of our separation of the spectrum into components are presented in Fig. 8; the diamonds denote the initial spectrum, crosses the spectrum of the variations, and squares the residual spectrum, which, in turn, consists of two components. Both components have spectra close to that of a spherically symmetric, homogeneous source; the low-frequency component has a maximum at about 1.5 GHz and an optically thin spectral index of about –0.7. Note that, according to [1], the integrated flux of the source in July 1988 did not exceed 80 mJy at 3.9 GHz. In the frequency range considered, only the optically thick part of the spectrum of the high-frequency component is observed; judging from its behavior, we expect that the maximum in the spectrum lies somewhere in the range 30–50 GHz.

We believe that the low-frequency component is a jet located at a considerable distance from the nucleus, which has already had time to evolve. Its spectral characteristics are similar to those of 0917 + 624, but it does not display any rapid variability.

5. CONCLUSION

We have observed rapid variability in the source 0524 + 034 with a timescale of about six days. The variations bear the character of shot noise and result from damping pulses of white noise with a limited spectrum.

The variations are correlated at all frequencies where the parameters of the variability could be determined, including in the optically thick part of the spectrum. In this part of the spectrum, we observe an increase of the correlation timescale.

We suggest that the variability is due to the illumination of inhomogeneities in the jet by a shock front passing through them and that the light curve reflects the distribution and characteristic sizes of these inhomogeneities (0.14–0.5 pc for angles to the line of sight not exceeding $10°$, a Lorentz factor $\gamma = 10$, and adopted redshift $z = 0.5$).

The simultaneity of the variations over a broad frequency range and the fact that the mean spectrum of the variable component coincides with the spectrum of a homogeneous, spherically symmetric source suggest the importance of acceleration of electrons and amplification of the magnetic field, whereas adiabatic expansion can be neglected.

In the variable component, we infer an initial electron spectrum with $\gamma = 1.4$. Therefore, this component should be located in the immediate vicinity of the "central engine."

In addition to the variable component, 0524 + 034 has two stationary or slowly varying components, one of which has $\gamma = 2.4$ in the optically thin part of the spectrum.

ACKNOWLEDGMENTS

REFERENCES

1. A. G. Gorshkov and V. K. Konnikova, Astron. Zh. **74**, 374 (1997).

2. V. R. Amirkhanyan, A. G. Gorshkov, and A. A. Kapustkin, Astron. Zh. **58**, 717 (1981).

3. R. Perley, private communication (1997).

4. D. R. Altschuler, Astron. J. **85**, 1559 (1980).

5. H. D. Aller, M. F. Aller, and P. E. Hodge, Astron. J. **86**, 325 (1981).

6. G. T. Romero, G. Surpi, and H. Vicetich, Astron. Astrophys. **301**, 64 (1995).

7. S. J. Qian, A. Quirrenbach, A. Witzel, *et al.*, Astron. Astrophys. **241**, 15 (1991).

8. I. S. Shklovskiĭ, Astron. Zh. **37**, 256 (1960).

9. H. Van der Laan, Nature **211**, 1131 (1966).

10. A. P. Marscher and W. K. Gear, Astrophys. J. **298**, 114 (1985).

11. N. S. Soboleva, A. V. Temirova, and T. B. Pyatunina, Preprint No. 32L (Special Astrophysical Observatory, 1986).

12. A. B. Berlin, A. A. Maksyasheva, N. A. Nizhel'skiĭ, *et al.*, *Abstracts of the XXVII Radio Astronomy Conference* [in Russian] (St. Petersburg, 1997), Vol. 3, p. 115.

13. A.M. Botashev, A. G. Gorshkov, V. K. Konnikova, and M. G. Mingaliev, Astron. Zh. **76**, 723 (1999).

14. A. G. Gorshkov and O. I. Khromov, Izv. SAO **14**, 15 (1981).

15. G. A. Seielstad, T. J. Pearson, and A. C. S. Readhead, Publ. Astron. Soc. Pacif. **95**, 842 (1983).

16. J. H. Simmonetti, J. M. Cordes, and D. S. Heeschen, Astrophys. J. **296**, 46 (1985).

17. P. A. Hughes, H. D. Aller, and V. F. Aller, Astrophys. J. **396**, 469 (1992).

18. E. Valtaoja, S. Haarala, H. Lehto, *et al.*, Astron. Astrophys. **203**, 1 (1988).

19. A. G. Pacholczyk and J. S. Scott, Astrophys. J. **210**, 311 (1976).

20. M. V. Popov and Yu. Yu. Kovalev, Astron. Zh. **76**, 643 (1999).

Translated by G. Rudnitskiĭ